

# MATHEMATICAL MODELING AND DYNAMIC DEVELOPMENT DESIGN OF AFAM POWER GAS TURBINE PLANT BY TRANSFORMATIVE DATA: CLUE ON AMBIENT FACTOR, ENERGY, AND FISCAL MATTERS

Samuel H. Kwelle<sup>1</sup> Nnadikwe Johnson<sup>2</sup> Ewelike Asterius Dozie<sup>3</sup> Chuku Dorathy E. Jerry<sup>4</sup>

<sup>1</sup> First Independent Power Limited, Rivers State, Nigerian

<sup>2</sup> Department of Petroleum and Gas Engineering Imo State University, Owerri, Nigeria

<sup>3</sup> H.O.D department of Agriculture and Environmental Engineering, Imo State University, Owerri, Nigeria

<sup>4</sup> Department of Petroleum and Gas Engineering Federal University Otuoke Bayelse State

## ABSTRACT

*This article evaluates the multi-objective performance of meffio technology using NSGA-II data to measure its energy, economic, and environmental performance. Two objective functions are shown. Cost of the environmental effect is placed second after overall cost rate. Both with and without the air preheater, objective function optimization has already been carried out. The air preheater decreased both desired functions. In the best case scenario, cycle without air preheater costs 30% more overall and costs the environment 33% more than cycle with air preheater. A sensitivity analysis of fuel unit cost was also performed. The total cost rate was higher and Pareto solutions were more sensitive to fuel unit cost at the lowest attainable environmental cost rate. The combustor loses the greatest energy (around 73%) when tested for energy losses across a number of components. The ambient temperature has an impact on the exergy losses and efficiency of various elements. All parts' exergy efficiency decreased as ambient temperature increased, and exergy losses increased. Energy efficiency drops as ambient temperature rises, going from 51% to 49% for a rise from 293 to 323 Kelvin.*

Keywords: Gas Turbine, Exergy, Sensitive, Environmental, meffio technology

## INTRODUCTION

The focus of research has been on high-efficiency, low-pollution systems because of the impact on the environment and rising energy prices. Another problem is how global warming affects the environment. Gas turbines are used to create industrial energy. Investigations in thermodynamics, the environment, and the economy are required for the gas turbine cycle. In order to determine how the ambient temperature influences irreversibility and second law performance, Kopac and Hilaci (2007) examined a Turkish thermal power plant [1]. In 2008, the author improved a CHP system. 15 kg of saturated steam are generated at 2.5 Bars by a 50 MW plant [2]. hyaei and others. [3] investigated the first and second law efficiencies of an Iranian gas turbine power plant's intake fogging system. Ahmadi et al. (2011) evaluated the environment, exergy, and exergoeconomics of combined cycle power plants [4]. A dual-pressure CHP system was examined by GanjehKaviri et al. (2012) [5]. A cogeneration system [2] was optimized by Ahmadi et al. [6]. Energy from polygeneration power plants was studied and optimized by Ahmadi et al. (2012) [7]. Shirazi et al. (2012) looked at the gas turbine cycle with internal reforming and fuel cell. Ahmadi et al. modeled and optimization of a multigenerational energy system. Memon et al. modeled the gas turbine cycle. They looked at CO<sub>2</sub> emissions and cycle efficiency as major performance metrics [10]. Reduced gas turbine compressor intake air temperature was achieved by MajdiYazdi et al. (2015) [11]. First and second law efficiency as well as net output power were studied by Ehyaei et al. [12]. An organic Rankine cycle system with a

gas turbine was investigated by Khaljani et al. (2015) [13]. Exergy, economic, and environmental evaluations of power-generating systems are examined in several research [3, 11, 12, 14–45].

No research has compared gas turbine optimization with and without air preheater. Others have only studied one gas turbine power facility. This research analyzed a power plant meffio technology

Using multi-objective genetic data, this study examines the thermodynamic, exergy economic, and exergy environmental performance of the Meffio technology gas turbine power plant (Niger Delta Area, Nigeria) (NSGA-II). Each generator produces 150 MW. This six-unit facility produces 900MW. Climate around the power facility is mild and humid. This inquiry is driven by two goals. The overall cost rate is first calculated, taking into account fuel, investment, and maintenance. Cost to the environment is one of the objective functions. Compressor, combustion chamber, gas turbine, and air heater are all parts of the cycle. The air compressor pressure ratio ( $r$ ), combustion chamber intake temperature ( $T$ ), and gas turbine inlet temperature ( $T$ ) were the main subjects of this investigation (). Two objective functions were affected by air preheaters. Four design variables are present in the second scenario, which does not use an air preheater: the compressor and turbine isentropic efficiencies, the gas turbine intake temperature, and the air compressor pressure ratio. Sensitivity analysis and fuel cost per unit of energy were also covered. Changes in intake air temperature have an impact on part destruction and energy efficiency. This synopsis contains:

- Analyzing gas turbine cycle exergy, exergy economic, and exergy environmental data with MATLAB
- Comparing objective function values for gas turbine cycle with and without air preheater.
- Impact of fuel cost per unit of energy on target functions
- Calculating cycle exergy loss
- Examining the influence of ambient temperature on each part's exergy efficiency, total exergy efficiency, and exergy destruction.

## MATHEMATICAL MODELING

### Analyzing energy

Thermodynamic modeling has been done for the process. The mass-energy balance equations for each component and the first law of thermodynamics are used in this modeling. In this research, we presupposed:

- Ideal air and exhaust gases are assumed.
- Air compressor inlet air temperature is 298 K and pressure is 1.013 bar [6].
- All cycle components are steady-state.
- 5% pressure reduction in air preheater for air, 3% for combustion products [6].
- Combustion chamber heat loss equals 5% low fuel heating value [6].
- $C_p$  is temperature-invariant.

Figures 1 and 2 depict a gas turbine cycle using Meffio technology with and without an air preheater. Figures demonstrate air compressor usage (AC). Natural gas and compressed air react in the combustion chamber (CC). To generate power, hot combustion chamber exhaust gas drives a gas turbine (GT). Gas turbine exhaust warms compressed air before it enters the combustion chamber in a cycle with an air preheater (APH).

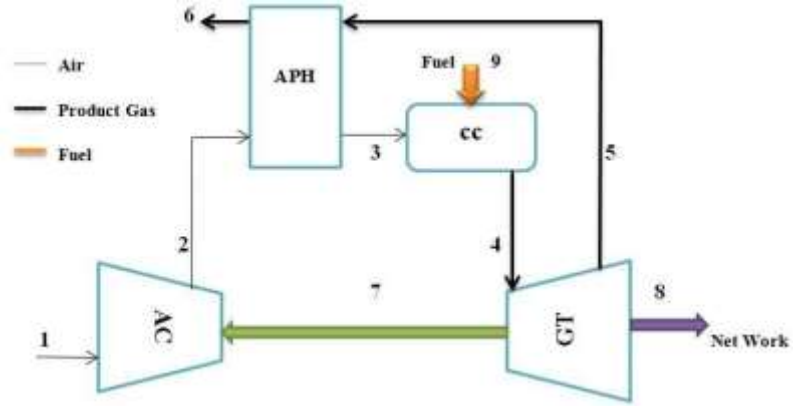


Figure 1. Power station fueled by gas turbines in meffio technology

meffio technology gas-turbine-powered power plant.:

Air compressor:

$$T_2 = T_1 \left\{ 1 + \frac{1}{\eta_{AC}} \left[ \frac{P_2}{P_1} \right]^{\frac{\gamma_a - 1}{\gamma_a}} - 1 \right\} \quad (1)$$

$$\dot{W}_{AC} = \dot{m}_a c_{p,a} (T_2 - T_1) \quad (2)$$

Where  $W_{AC}$  is the pneumatics network in the given equation.

Air preheater:

$$\dot{m}_a c_{p,a} (T_3 - T_2) = \dot{m}_g c_{p,g} (T_5 - T_6) \quad (3)$$

$$P_3 = P_2 (1 - \Delta P_{a,APH}) \quad (4)$$

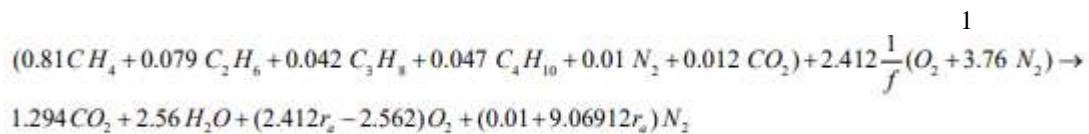
$$P_6 = P_5 (1 - \Delta P_{g,APH}) \quad (5)$$

Combustor

$$\dot{m}_a h_3 + \dot{m}_f LHV = \dot{m}_g h_4 + (1 - \eta_{CC}) \dot{m}_f LHV, \quad \eta_{CC} = 0.95 \quad (6)$$

$$P_4 = P_3 (1 - \Delta P_{CC}) \text{ with } \Delta P_{CC} = 0.05 \text{ Bar} \quad (7)$$

In this context, LHV refers to the 50,000 (kJ/kg) thermal efficiency that has been assumed for methane as a fuel. Combustor chemistry looks like this:



The preceding formula has the fuel-to-air molar ratio,  $f$ , as an input.

$$f = \frac{n_{fuel}}{n_{air}} \tag{8}$$

The mass ratio may be found by taking the molar ratio and multiplying it by the molar mass. Gas turbine:

$$T_5 = T_4 \left\{ 1 - \eta_{GT} \left[ 1 - \left[ \frac{P_4}{P_5} \right]^{\frac{1-\gamma_g}{\gamma_g}} \right] \right\} \tag{9}$$

$$\dot{W}_{GT} = \dot{m}_g c_{p,g} (T_4 - T_5) \tag{10}$$

$$\dot{m}_g = \dot{m}_a + \dot{m}_f \tag{11}$$

$$\dot{W}_{net} = \dot{W}_{GT} - \dot{W}_{AC} \text{ with } \dot{W}_{net} = 150 \text{ MW} \tag{12}$$

The previous equations "define the isentropic efficiency of a gas turbine," where "W" and "W" are respectively the network and cycle of the gas turbine and cycle, respectively, in metric megawatts (MW). The aforementioned equation can be solved to determine the traits and thermodynamic values of the individual portions. Figure 2 depicts and describes the second cycle under examination (without an air preheater):

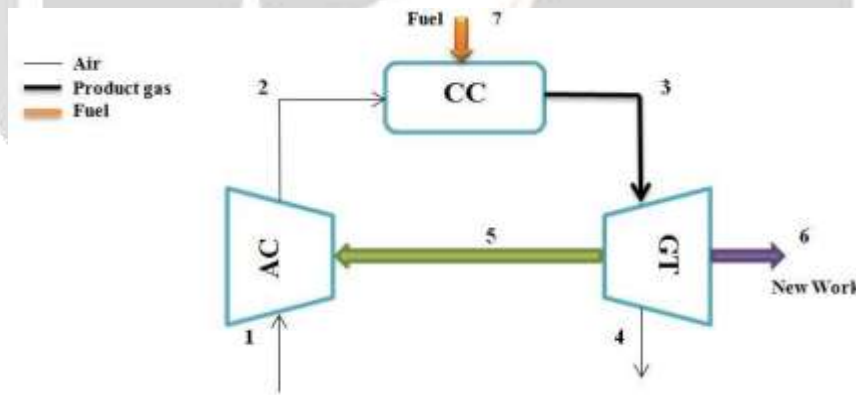


Figure 2. meffio technology air-less gas turbine cycle

ANALYSIS OF EXERGY

Exergy can be classified as physical, chemical, kinetic, or potential. Kinetic and prospective exergies are ignored here because they have little impact on system analysis. Combining the first and second laws of thermodynamics, the following exergy balance is created. The exergy balance equation is as follows [46]:

$$\dot{E}x = \dot{E}x_{ph} + \dot{E}x_{ch} \tag{13}$$

Exergy per mass unit formulae for physics and chemistry[46]:

$$ex_{ph} = (h - h_0) - T_0(s - s_0) \tag{14}$$

Furthermore, we may express the exergy of a mixture as a function of mass using [46]:

$$ex_{mix}^{ch} = \left[ \sum_{i=1}^n X_i ex^{ch_i} + RT_0 \sum_{i=1}^n X_i \ln X_i \right] \tag{15}$$

Table 1 summarizes the efficiency and exergy destruction equations for the various parts of the gas turbine cycle.

Table 1. Complete-system exergy-destruction and performance equations

Components	Cycle	Exergy efficiency (%)	Exergy destruction (MW)
Air compressor	With APH	$\eta_{ex,AC} = \frac{\dot{E}_2 - \dot{E}_1}{\dot{W}_{AC}}$	$\dot{E}_{D,AC} = \dot{E}_1 - \dot{E}_2 - \dot{W}_{AC}$
	Without APH	$\eta_{ex,AC} = \frac{\dot{E}_2 - \dot{E}_1}{\dot{W}_{AC}}$	$\dot{E}_{D,AC} = \dot{E}_1 - \dot{E}_2 - \dot{W}_{AC}$
Combustion chamber	With APH	$\eta_{ex,CC} = \frac{\dot{E}_4}{\dot{E}_3 + \dot{E}_9}$	$\dot{E}_{D,CC} = \dot{E}_3 + \dot{E}_9 - \dot{E}_4$
	Without APH	$\eta_{ex,CC} = \frac{\dot{E}_3}{\dot{E}_2 + \dot{E}_7}$	$\dot{E}_{D,CC} = \dot{E}_2 + \dot{E}_7 - \dot{E}_3$
Gas turbine	With APH	$\eta_{ex,GT} = \frac{\dot{W}_{GT}}{\dot{E}_4 - \dot{E}_5}$	$\dot{E}_{D,GT} = \dot{E}_4 - \dot{E}_5 - \dot{W}_{GT}$
	Without APH	$\eta_{ex,GT} = \frac{\dot{W}_{GT}}{\dot{E}_3 - \dot{E}_4}$	$\dot{E}_{D,GT} = \dot{E}_3 - \dot{E}_4 - \dot{W}_{GT}$
Air preheater	With APH	$\eta_{ex,APH} = 1 - \left( \frac{\dot{E}_{D,APH}}{\sum_{i,APH} \dot{E}_i} \right)$	$\dot{E}_{D,APH} = (\dot{E}_2 + \dot{E}_5) - (\dot{E}_3 + \dot{E}_6)$
	Without APH	-	-

ANALYZING EXERGO-ECONOMIC

Exergy-economics is a novel idea that was created in order to create a system that was more economical and effective. This concept was first put forth by Valero and his collaborators in [47]. Finding out how much money is needed to be spent for a specific level of exergy in a flow is the aim of an exergy-economics study. An effective indicator for studying and enhancing the economic cycle is the exergy cost of goods. A system's cost-benefit analysis looks like this [47, 48]:

$$\sum_e \dot{C}_{e,k} + \dot{C}_{w,k} = \dot{C}_{q,k} + \sum_i \dot{C}_{i,k} + \dot{Z}_k \tag{16}$$

The coordinates may be calculated using Equation 16 [47, 48]:

$$\sum (c_e \dot{E}x_e)_k + c_{w,k} \dot{W}_k = c_{q,k} \dot{E}x_{q,k} + \sum (c_l \dot{E}x_l)_k + \dot{Z}_k \tag{17}$$

$$\dot{C}_j = c_j E_j \tag{18}$$

$c$  stands for the exergy unit cost associated with the input (\$ / MJ),  $c$  stands for the exergy unit cost associated with the output (\$ / MJ),  $c$ , stands for the cost rate associated with the Kth flow line (\$ / MJ), and  $c$ , stands for the exergy unit cost associated with the heat associated with the Kth flow line (\$ / MJ) in the aforementioned formulas.  $C$  and  $c$  are abbreviations that stand for the flow cost rate and the exergy unit cost, respectively, for the flow line. There is no connection between any of the components in Equation 15 and the rate at which exergy is lost. It is possible to calculate the price of the exergy destruction rate by combining the exergy balancing equation with the exergy economic equation.

$$\dot{E}x_{F,k} = \dot{E}x_{p,k} + \dot{E}x_{D,k} \tag{19}$$

$$\dot{C}_{F,k} = c_{F,k} \dot{E}x_{D,k} \tag{20}$$

$$\dot{C}_{P,k} = c_{P,k} \dot{E}x_{D,k} \tag{21}$$

Where  $C$  and  $C$  are rates in dollars per second for the cost of fuel and goods, respectively. Exergy rates and cost balance equations may be solved for each part of the system if their respective costs are known. Investing and maintaining each component's value is represented by  $Z$  in Equation 16. A stream price rate has also been defined for each line. The following equations are used to determine the exergy destruction cost rate:

$$\dot{C}_{D,k} = c_{F,k} \dot{E}x_{D,k} \tag{22}$$

The three variables in this equation are the exergy destruction rate, denoted by  $E_x$ , (\$/s), the exergy unit cost for input routes in the kth subsystem, denoted by  $c$ , (\$/MJ), and the exergy destruction cost rate in the kth subsystem. The investment cost has been calculated using the following equation [47, 48], which takes into account both the equipment's purchase price and ongoing maintenance costs[47, 48] :

$$\dot{Z}_k = Z_k CRF \phi / (N \times 3600) \tag{23}$$

The following formula includes the cost of the kth component, denoted by  $Z$ , in US dollars; the corresponding component-specific formulae are tabulated in Table 2. The constants used in the Table 2 equations have been moved to Table 3 as well. In this piece, we take to be 1.06 [48], which is the maintenance coefficient,  $\phi$ . In this analysis,  $N$  represents the number of hours per year that a power plant is operational (8,000), and  $CRF$  is the return on capital coefficient, which has been set at 0.182 (based on [47, 48]). The gasoline cost rate is determined by the following equation [47, 48]:

$$\dot{C}_f = c_f \dot{m}_f LHV \tag{24}$$

In the equation shown above,  $C$  represents the cost of fuel per unit of energy, which is equal to 0.004 (US\$/MJ) [48]. Meanwhile,  $\dot{m}$  represents the fuel mass flow rate in kilograms per second.

Table 2. Detailed cost functions for every component of the system

System Components	Capital or investment cost functions
Air compressor	$Z_{AC} = \left( \frac{C_{11}\dot{m}_a}{C_{12} - \eta_{AC}} \right) \left( \frac{P_2}{P_1} \right) \ln \left( \frac{P_2}{P_1} \right)$
Combustion chamber	$Z_{CC} = \left( \frac{C_{21}\dot{m}_a}{C_{22} - \frac{P_4}{P_3}} \right) [1 + \text{EXP}(C_{23}T_4 - C_{24})]$
Gas turbine	$Z_{GT} = \left( \frac{C_{31}\dot{m}_g}{C_{32} - \eta_{GT}} \right) \ln \left( \frac{P_4}{P_5} \right) [1 + \text{EXP}(C_{33}T_4 - C_{34})]$
Air preheater	$Z_{APH} = C_{41} \left( \frac{\dot{m}_g(h_5 - h_6)}{(U)(\Delta TLM)} \right)^{0.6}$

Table 3. Constants that were used in the equations shown in Table 2

System Components	Constants
Air compressor	$C_{11} = 39.5 \text{ US\$ / (kg/s) } , C_{12} = 0.9$
Combustion chamber	$C_{21} = 25.6 \text{ US\$ / (kg/s) } , C_{22} = 0.995$ $C_{23} = 0.018 \text{ K}^{-1} , C_{24} = 26.4$
Gas turbine	$C_{31} = 266.3 \text{ US\$ / (kg/s) } , C_{32} = 0.92$ $C_{33} = 0.036 \text{ K}^{-1} , C_{34} = 54.4$
Air preheater	$C_{41} = 2290 \text{ US\$ / m}^{1.2} , U = 0.018 \text{ kW / (m}^2\text{K)}$

EXERGY ENVIRONMENTAL SYSTEMS ANALYSIS

Researchers are interested in improving power production systems, as well as reducing fuel consumption and environmental impact, as ways to lighten the load on the world. As a result, improving heating systems to fulfill demands has become an urgent issue in recent years. One of the key objectives of this effort is to better understand the harmful impacts of CO and NOx emissions. The primary zone of the combustion process's adiabatic combustion temperatures are calculated using the following equation [8, 49].

$$T_{pz} = A\sigma^\alpha \exp(\beta(\sigma + \lambda)^2) \pi^{x^*} \theta^{y^*} \psi^{z^*} \tag{25}$$

in this equation,  $\pi$  represents the dimensionless pressure ( $P/P_{ref}$ ), and  $\theta$  represents the dimensionless temperature ( $T/T_{ref}$ ). Also,  $\psi$  is the atomic ratio (H/C), and if  $\phi \leq 1$ , we have  $\sigma = \phi$  ( $\phi$ , is the mass or molar ratio), but if is greater than one, then we get  $\sigma = \phi - 0.7$ .

In addition, x, y, and z are examples of quadric functions of  $\sigma$ .

$$x^* = a_1 + b_1\sigma + c_1\sigma^2 \tag{26}$$

$$y^* = a_2 + b_2\sigma + c_2\sigma^2 \tag{27}$$

$$z^* = a_3 + b_3\sigma + c_3\sigma^2 \tag{28}$$

The constants  $A, \alpha, \beta, \lambda, a, b, c$  in the aforementioned equations. In Table 4 [8, 49] we can see these constants. As the flame temperature in an adiabatic combustion chamber rises or falls, different amounts of carbon monoxide and nitrogen oxide are produced. The following equation is used to determine the quantity of pollution (g/kg of fuel) [8, 49]:

$$\dot{m}_{NOx} = \frac{0.15 \times 10^{16} \times \tau^{0.5} \times \exp(-71100/T_{pz})}{P_3^{0.05} \times (\Delta P/P)} \tag{29}$$

$$\dot{m}_{CO} = \frac{0.179 \times 10^9 \times \exp(7800/T_{pz})}{P_3^2 \times \tau \times (\Delta P/P)} \tag{30}$$

The time spent in the combustion zone, according to the equations above, is, and 0.002 seconds has been recognized as a credible approximation [8, 49]. P3 is the pressure at the combustion chamber's entry in this equation, and (P/P) represents the dimensionless pressure loss within the chamber.

Table 4. Constants that are used throughout equations 24-27

Constants	0.3 ≤ φ ≤ 1.0		1.0 ≤ φ ≤ 1.6	
	0.92 ≤ θ ≤ 2	2 ≤ θ ≤ 3.2	0.92 ≤ θ ≤ 2	2 ≤ θ ≤ 3.2
A	2361.7644	2315.7520	916.8261	1246.1778
α	0.1157	-0.0493	0.2885	0.3819
β	-0.9489	-1.1141	0.1456	0.3479
λ	-1.0976	-1.1807	-3.2771	-2.0365
a <sub>1</sub>	0.0143	0.0106	0.0311	0.0361
b <sub>1</sub>	-0.0553	-0.0450	-0.0780	-0.0850
c <sub>1</sub>	0.0526	0.0482	0.0497	0.0517
a <sub>2</sub>	0.3955	0.5688	0.0254	0.0097
b <sub>2</sub>	-0.4417	-0.5500	0.2602	0.5020
c <sub>2</sub>	0.1410	0.1319	-0.1318	-0.2471
a <sub>3</sub>	0.0052	0.0108	0.0042	0.0170
b <sub>3</sub>	-0.1289	-0.1291	-0.1781	-0.1894
c <sub>3</sub>	0.0827	0.0848	0.0980	0.1037

**CONDITIONS OF OBJECTIVE FUNCTION**

In this study, both objective functions have been considered. The cost of fuel, investments, maintenance, and exergy destruction are all included in the first objective function, as indicated below[47, 48]:

$$\dot{C}_{Tot} = \dot{C}_f + \sum \dot{Z}_k + \sum \dot{C}_{D,k} \tag{31}$$

In this equation,  $\dot{C}_f$ ,  $\dot{Z}_k$  and  $\dot{C}_{D,k}$  stand for the cost of fuel, the cost of purchasing equipment, and the cost rate of exergy destruction, respectively.

The rate at which exergy is destroyed may be calculated using the following equation[47, 48]:

$$\dot{C}_{D,k} = c_{F,k} \dot{E}x_{D,k} \tag{32}$$

The exergy destruction price rate in the kth subsystem is denoted by C<sub>D,k</sub>, (\$/s), the exergy unit cost for input routes in the kth subsystem is denoted by c<sub>F,k</sub>, (\$/MJ), and the exergy destruction rate in the kth subsystem is denoted by Ex<sub>D,k</sub> (\$/s). Cost of environmental effect is the second objective function, and it is determined by

multiplying the unit damage costs (in US dollars per second) of carbon monoxide and nitrogen oxide emissions. The unit damage cost values are as follows [8, 49 ]:

$$C_{CO} = 0.02086 \text{ US\$/kgCO} \quad (33)$$

$$C_{NOx} = 6.853 \text{ US\$/kgNOx} \quad (34)$$

As a result, the following should serve as the second objective function:

$$\hat{C}_{env} = C_{CO}\dot{m}_{CO} + C_{NOx}\dot{m}_{NOx} \quad (35)$$

Both of the goal functions that are being looked at in this essay need to be scaled down.

## TECHNIQUE FOR OPTIMIZING PERFORMANCE

### COMBINATORIC OPTIMIZATION

A common example of an optimization problem is choosing the best answer (or answers) from a list of candidates while keeping the optimization of a particular criterion in mind. Multi-objective optimization aims to find the Pareto optimal solutions to the objective function. Additionally, it belongs to the broader category of multi-criteria decision-making approaches, which also includes a wide range of alternative evaluations. There are numerous conflicting goals in these problems as opposed to a single optimal solution, which makes them different from single-objective optimization problems. In multi-objective optimization, a set of viable alternatives is compared to the best solutions. Multi-objective optimization has the great property that no solution is superior to any other solution, and alternatives may be assessed for the problem based on the specifications of each Pareto solution.

### DIFFERENTIAL GENETIC INFORMATION (NSGA-II)

Previously single-objective genetic data has been turned into multi-objective data that offers a Pareto Front of optimal choices rather than a single best answer by including these two key operators. The population can be divided into subsets, the first of which includes everyone who has not yet received a nomination from another person. The members of each group are ranked according to the number of groupings, with the first group's members completely dominating the second group. A general flowchart of multi-objective genetic data for the National Sustainable Agriculture Alliance II is shown in Figure 3[50]. (NSGA-II).

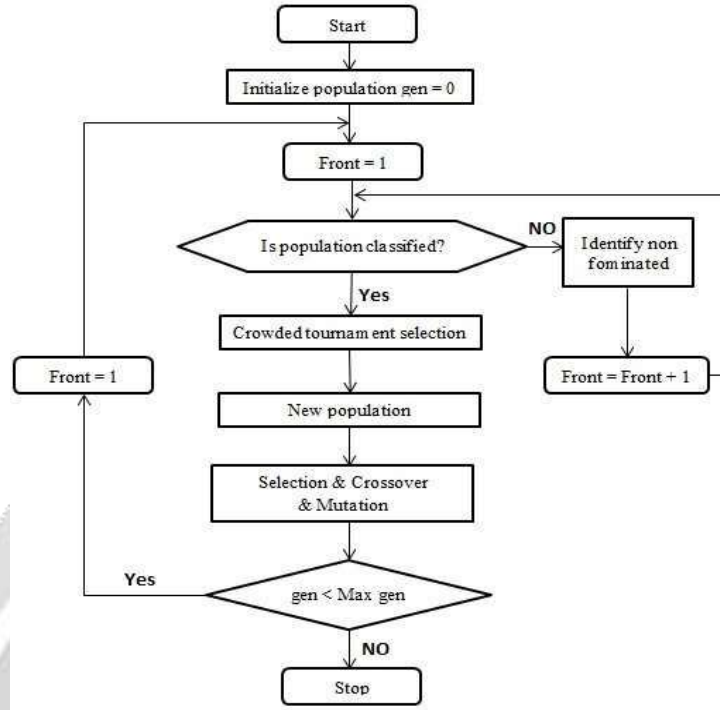


Figure 3. NSGA-II data Flow chart

RESULTS

DESIGN FACTORS

100 years for the generation and 200 years for the population, correspondingly. From 0.01% to 0.90% of mutations were possible. The iteration process will come to an end if 500 iterations go by without convergence. For the first case cycle, which is the gas turbine cycle with an air preheater, this work considers the air compressor pressure ratio ( $r$ ), combustion chamber inlet temperature ( $T$ ), gas turbine intake temperature ( $T$ ), air compressor isentropic efficiency ( $\eta$ ), and gas turbine isentropic efficiency ( $\eta$ ). A different test setup examines the cycle without performing the air preheating phase. In this case, the pressure ratio of the air compressor, the intake temperature of the gas turbine, and the isentropic efficiency of the air compressor and gas turbine are the design variables. The realistic restrictions that may be imposed for each design variable during optimization are shown in Table 5.

Table 5. constraints of the Model

Constraints	Reason
$6 \leq r_{AC} \leq 16$	Commercial availability
$800 K \leq T_3 \leq 1100 K$	Material limitation
$1200 K \leq T_4 \leq 1600 K$	Material limitation
$0.7 \leq \eta_{AC} \leq 0.9$	Commercial availability
$0.7 \leq \eta_{GT} \leq 0.92$	Commercial availability

The meffio technology power plant is used to verify simulation findings. Table 6 compares findings.

Table 6. A contrast between the actual data from the power plant and the simulation

Parameter	Power plant data	Simulation Code	Difference (%)
$\hat{C}_{Tot}$ (US\$/s)	2.82	2.98	4.6
$T_2$ (K)	606	612	1.0
$T_5$ (K)	864	879	1.7
$T_6$ (K)	672	695	3.4

Multi-objective genetic optimization results

Figure 4 shows the Pareto solution for a gas turbine plant using multi-objective genetic data. The study discovers that increased environmental costs result in decreased overall costs. Figure demonstrates that the overall cost rate drops with a steeper slope from 0.06 (US\$/s) to 0.1 (US\$/s). The overall cost decreases from 0.1 (US\$/s), but the environmental cost increases significantly. Every Pareto-optimal solution exists. The ideal strategy is determined by the designer's perspective and the importance of each desired function. A, B, and C are shown in the illustration. The cost of A is the greatest overall and the cheapest for the environment. The environmental and total expenses are lowest at Point C. Point B is the best option because it simultaneously optimizes both objective functions.

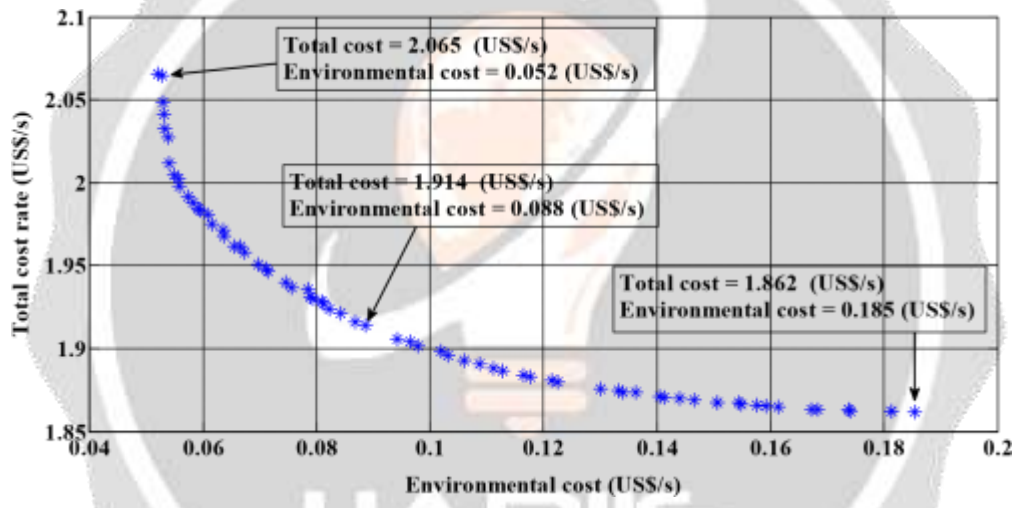


Figure 4. NSGA-II data led to the Pareto optimal solution for the meffio technology gas turbine power facility.

In the second scenario, the meffio technology's air preheater is disabled in order to examine the impact that this removal has on objective functions. Figure 5 depicts the Pareto optimal strategy, which entails taking out the air preheater. Evidence supports options A, B, and C. In Figure 4, Point A has the lowest environmental cost while having the highest overall cost. Point C has the lowest costs overall and in terms of the environment. Both of the objective functions are enhanced by turning off the air preheater. The only cost rate at point C that is higher than the total cost rate is the environmental cost rate, as shown in Figure 4. The results show that installing an air preheater reduces both objective functions. Table 7 displays the A, B, and C values for both scenarios. The cycle without an air preheater is 30% more expensive overall and 33% more expensive environmentally at the ideal point when compared to the cycle with an air preheater (point B).

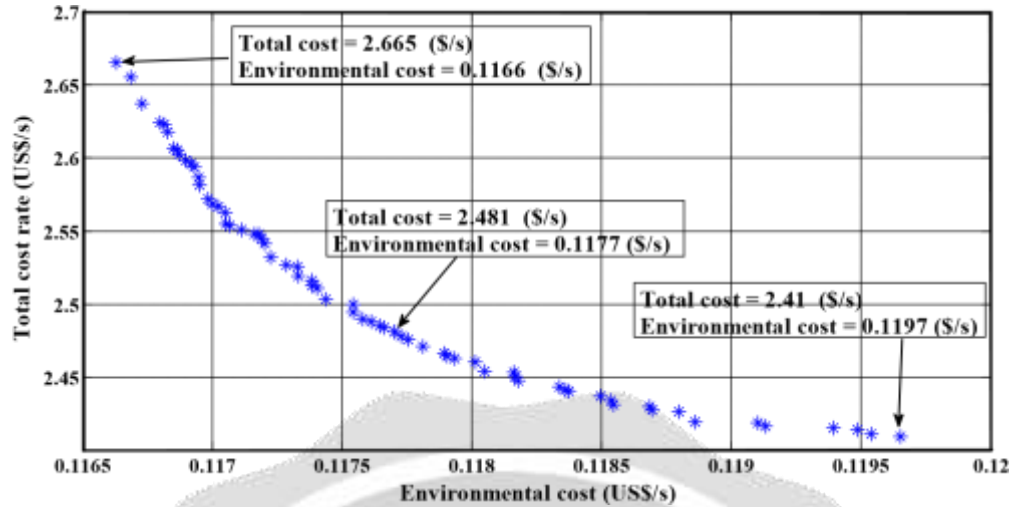


Figure 5. NSGA-II data Pareto solution for meffio technology without air preheater

Table 7. Point-by-point values of the goal function for the two cycles under consideration

Cases	Objective function	A point	B point	C point
Aliabad power plant cycle	Total cost rate (US\$/s)	2.065	1.914	1.862
	Environmental cost (US\$/s)	0.052	0.088	0.185
Aliabad power plant cycle without air preheater	Total cost rate (US\$/s)	2.665	2.481	2.41
	Environmental cost (US\$/s)	0.1166	0.1177	0.1197

VARIABLE DISTRIBUTION

Figures 6a through 10e show the different distributions. Upper and lower design parameters are indicated by dashed lines. Pareto solutions for compressor pressure ratio are shown in Figure 6a. According to this distribution, modifying this variable inside the specified range is incompatible with both goal functions. The Pareto distributions for combustion chamber and gas turbine intake temperatures are shown in Figures 6b and 6c. As can be seen, Pareto solutions are almost at the maximum, which suggests that increasing the values of these two variables improved both objective functions. Intake temperatures for combustion chambers are typically 1005 Kelvin, whereas inlets for gas turbines generally 1470 Kelvin. Figures 6d and 6e show the design variable distributions for gas turbines and compressors, respectively. Inferring that these values have improved both objective functions, it can be seen from these two numbers that the majority of compressor isentropic efficiencies are around 87% and gas turbine isentropic efficiencies are over 90%.

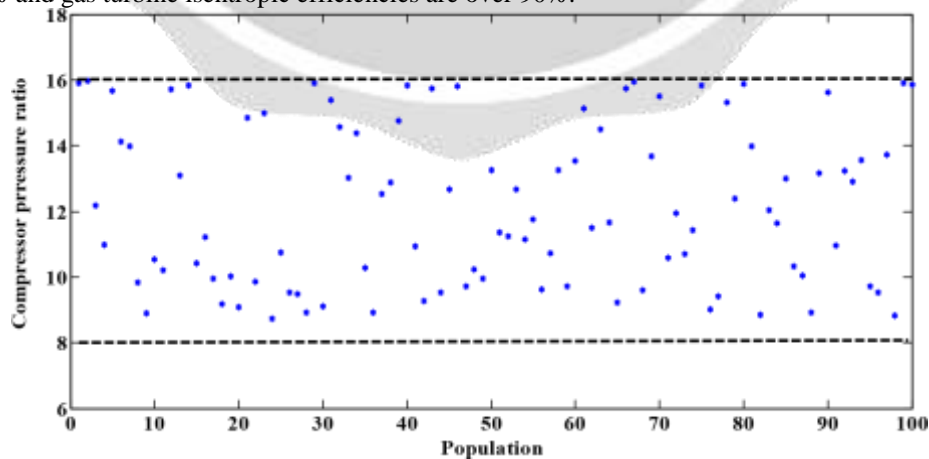


Figure 6a. The Pareto solution for the distribution of values for the compressor pressure ratio

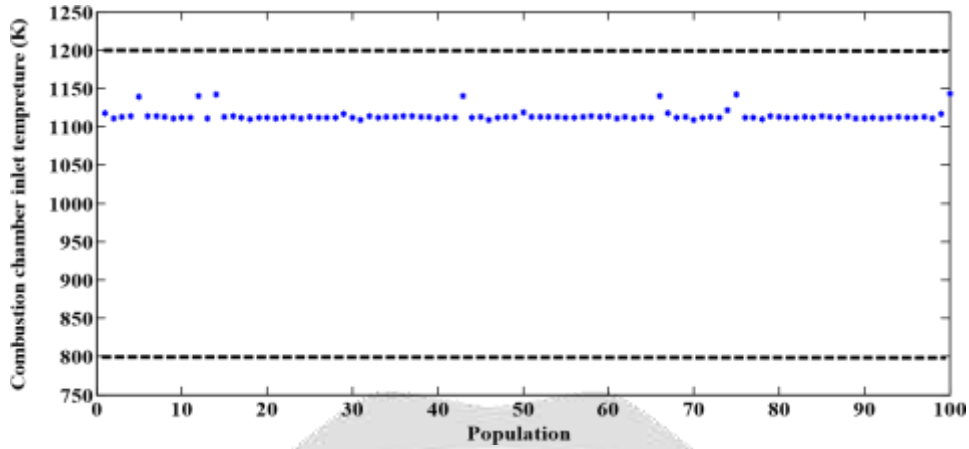


Figure 6b. Pareto chart showing the distribution of temperature values at the intake of the combustion chamber

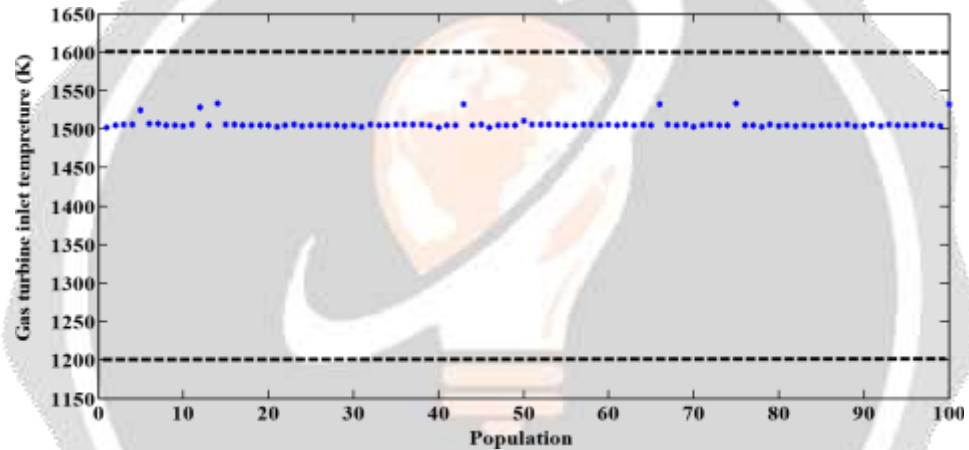


Figure 6c. The Pareto solution for the distribution of temperature values at the intake of gas turbines

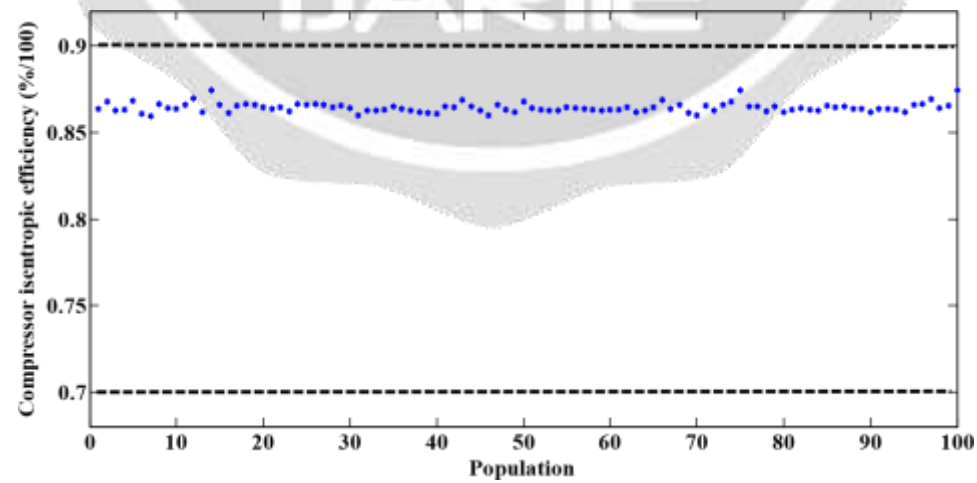


Figure 6d. Pareto analysis showing the distribution of efficiency ratings for air compressors

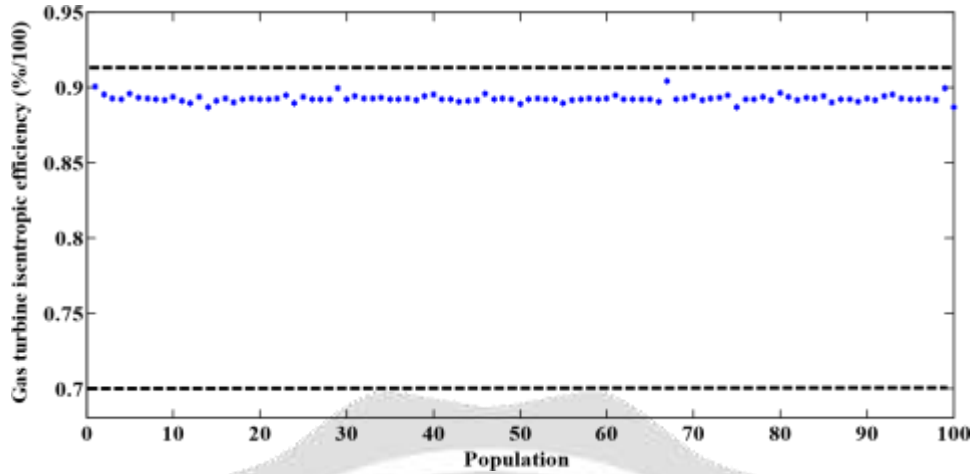


Figure 6e. Values of efficiency distribution for gas turbines according to the Pareto principle

Table 8. Parameter of design value at A, B, and C

Parameter	Point A	Point B	Point C
$r_{AC}$	12.1	9.3	11.6
$T_3$	1119	1121	1128
$T_4$	1511	1504	1505
$\eta_{AC}$	88.1	87.4	87.2
$\eta_{GT}$	89.8	89.1	89.3

ANALYSIS OF SENSITIVITY

The relationship between the cost of fuel per unit of energy and the sensitivity of various objective functions is shown in Figure 7. This graph demonstrates that in the areas of the graph where the total cost rate is lower, the sensitivity of Pareto solutions to the fuel unit cost is larger. We may say that the cost of environmental effects is only slightly responsive to changes in the fuel unit cost parameter.

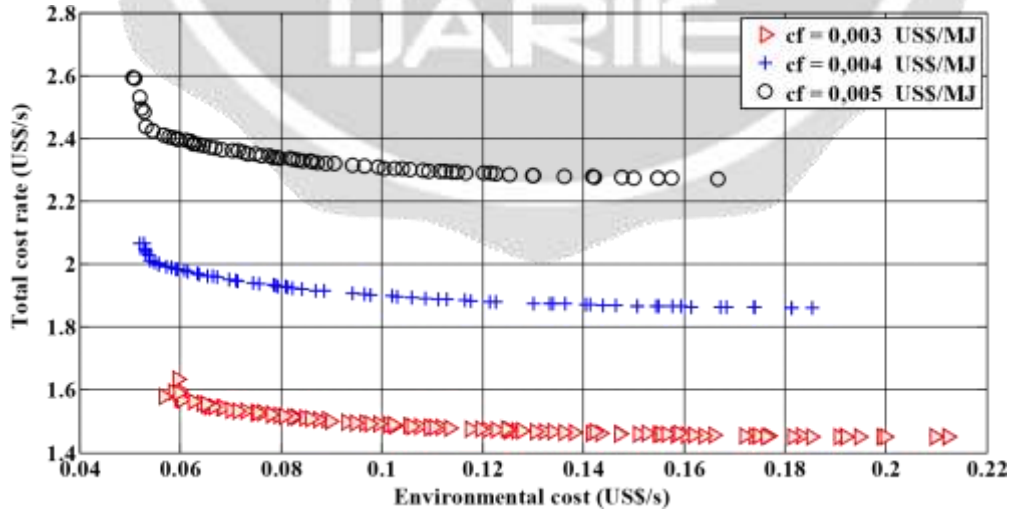


Figure 7. sensitivity of the Pareto solution to changes in the cost of fuel per energy unit

**EXERGY DESTRUCTION**

Figure 8 displays energy destruction levels at various stages of the cycle. We can deduce from this data that the combustion chamber directly causes the highest rate of energy destruction. The three irreversible processes that cause exergy depreciation are heat transmission, friction, and chemical reaction. Figure 9 depicts the percentage of energy lost during the course of the cycle. This information indicates that the combustion chamber accounts for roughly 73% of the entire exergy destruction. By raising the air's temperature before it enters the combustion chamber, lowering energy loss, and maximizing the air to fuel ratio, it can be decreased.

Figure 8. Exergy degradation values for varied sections

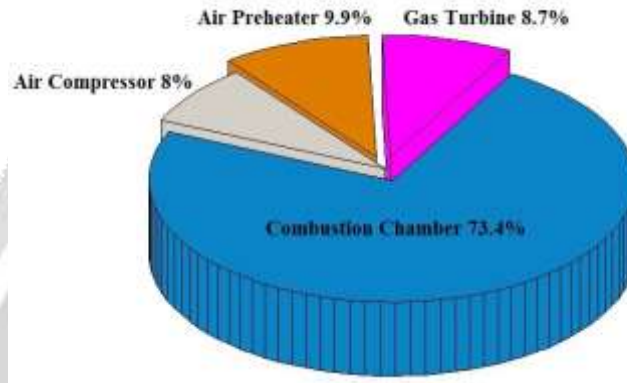


Figure 9. Exergy degradation percentage for various cycle sections

Figure 10 shows the connection between the temperature of the surrounding environment and the exergy efficiency of various components. It is easy to envision that the energy efficiency of every component would decrease as a result of an increase in the ambient temperature. Exergy efficiency of the air compressor, combustion chamber, gas turbine, and air preheater all decrease when the ambient temperature is raised from 293 to 323 Kelvin. The exergy efficiency of the air compressor decreases from 90% to 87.7%, the combustion chamber efficiency decreases from 51.9% to 48.6%, the gas turbine efficiency decreases from 85.4% to 81.4%, and the air preheater efficiency decreases from 93.9% to 90%.

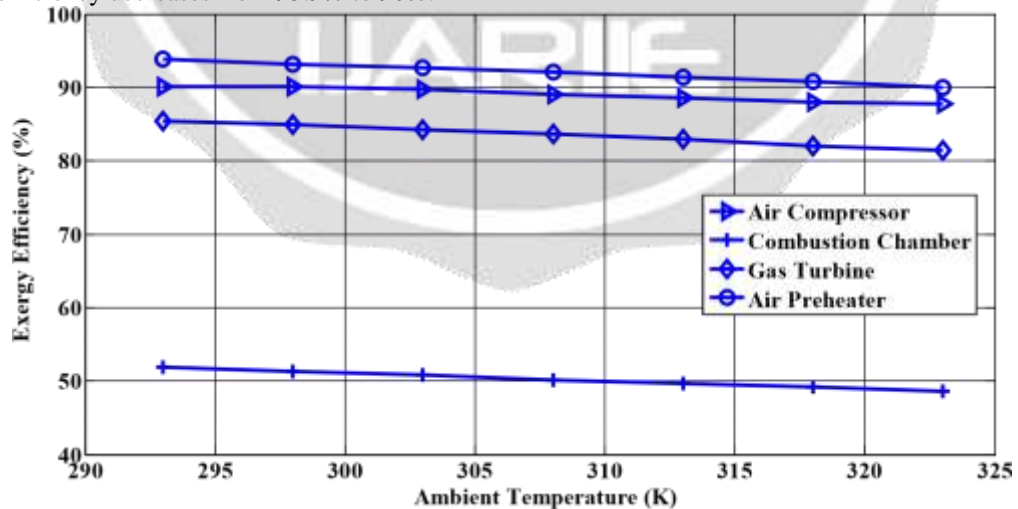


Figure 10. Variations in exergy efficiency across a variety of components in response to variations in ambient temperature

Figure 11 shows total exergy efficiency as a function of temperature change. As the temperature rises, total energy efficiency falls. The overall energy efficiency decreases from 1% to 4% as temperature increases from 293 to 323 K. This result implies that lower energy efficiency is a negative consequence of higher average temperatures.

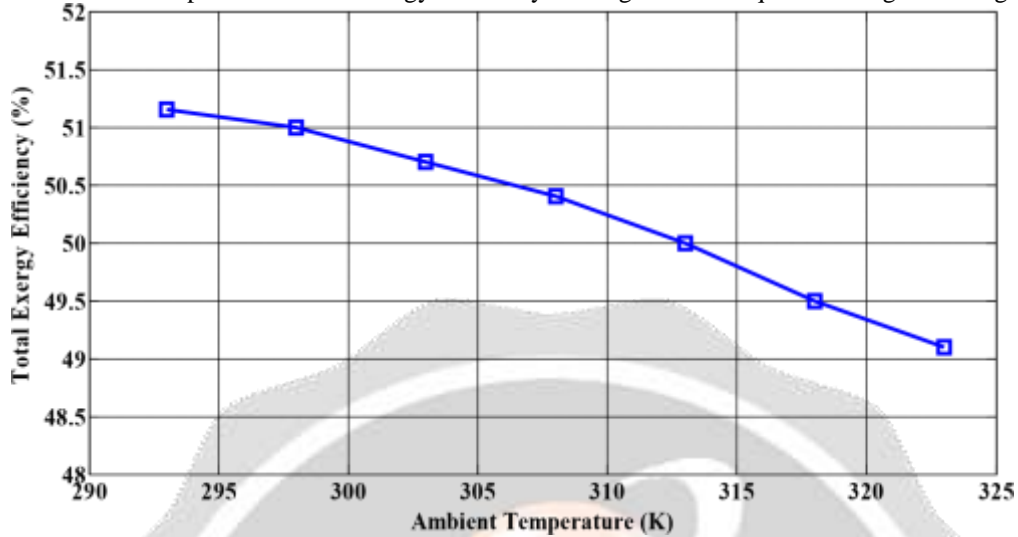


Figure 11. Variations in exergy efficiency in response to variations in the surrounding temperature

The correlation between energy destruction and ambient temperature is seen in Figure 12. The energy destruction caused by rising temperatures is shown in this image. Air compressor, combustion chamber, gas turbine, and air preheater energy destruction rose by 14%, 0.6%, 18%, and 10%, respectively, when the ambient temperature was raised from 293 K to 303 K.

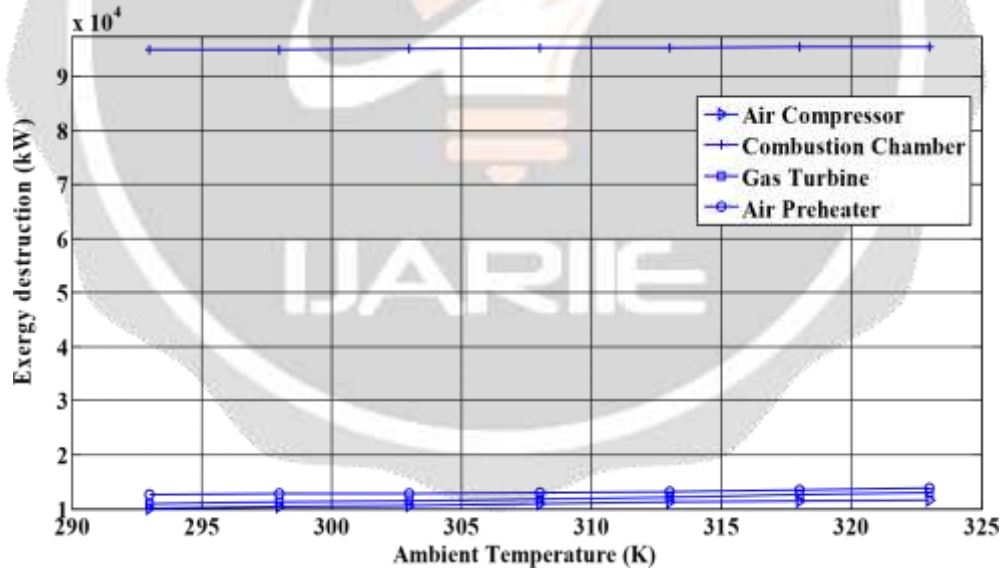


Figure 12. The amount of exergy that is destroyed varies during the cycle according to the various sections as ambient temperature changes.

CONCLUSION

The Niger delta region of Nigeria's Meffio Technology gas turbine power plant is researched in this study for its thermodynamic, economic, and environmental properties. Additionally, the plant is optimized with the aid of the MATLAB-written NSGA-II program. The two objective functions that were taken into consideration were the rate of the total cost and the cost of the impact on the environment. Additionally, this cycle's optimization has been carried out in two different setups, one with and one without an air preheater. Objective functions that were

sensitive to these kinds of fluctuations were also used to assess variations in the amount of money spent on fuel per unit of energy. Additionally, the effectiveness of the cycle's overall energy use as well as the effects of a change in the ambient temperature on each of its component parts were examined. Following is a summary of the outcomes that were found:

- The aim functions and total cost rate were reduced by the air preheater.
- The cycle with an air preheater has the lowest total cost and the lowest environmental cost at Point B in the Pareto optimal solution.
- The overall cost rate and the sensitivity of Pareto solutions to fuel price were higher in areas of the graph where environmental costs were lower. The combustion chamber was the source of the greatest exergy loss.
- As the temperature increased, every component's energy efficiency decreased.
- As the ambient temperature grew, more components began to degrade and become irreversible.

## ACKNOWLEDGEMENT

All the praise go to Almighty God, The most beneficent and merciful for blessing the authors, The authors would like to give a special thanks to the Johnson and Sylvester Centre for African Research Engineer Library, for their Assistance in utilizing of the centre for Africa Research Engineering Library equipment to actualize our detailed results.

## REFERENCES

- [1] Kopac M, Hilalci A. Effect of ambient temperature on the efficiency of the regenerative and reheat Çatalağzı power plant in Turkey. *Applied Thermal Engineering* 2007;27:1377–85. <https://doi.org/10.1016/j.applthermaleng.2006.10.029>.
- [2] Sahoo P. Exergoeconomic analysis and optimization of a cogeneration system using evolutionary programming. *Applied Thermal Engineering* 2008;28:1580–8. <https://doi.org/10.1016/j.applthermaleng.2007.10.011>.
- [3] Ehyaei M, Mozafari A, Alibiglou M. Exergy, economic & environmental (3E) analysis of inlet fogging for gas turbine power plant. *Energy* 2011; 36:6851–61. <https://doi.org/10.1016/j.energy.2011.10.011>.
- [4] Ahmadi P, Dincer I, Rosen MA. Exergy, exergoeconomic and environmental analyses and evolutionary data based multi-objective optimization of combined cycle power plants. *Energy* 2011;36: 5886–98. <https://doi.org/10.1016/j.energy.2011.08.034>.
- [5] Kaviri AG, Jaafar MNM, Lazim TM. Modeling and multi-objective exergy based optimization of a combined cycle power plant using a genetic data. *Energy Conversion and Management* 2012;58:94–103. <https://doi.org/10.1016/j.enconman.2012.01.002>.
- [6] Ahmadi P, Almasi A, Shahriyari M, Dincer I. Multi-objective optimization of a combined heat and power (CHP) system for heating purpose in a paper mill using evolutionary data. *International Journal of Energy Research* 2012;36:46–63. <https://doi.org/10.1002/er.1781>.
- [7] Ahmadi P, Rosen MA, Dincer I. Multi-objective exergy-based optimization of a polygeneration energy system using an evolutionary data. *Energy* 2012;46:21–31. <https://doi.org/10.1016/j.energy.2012.02.005>.
- [8] Shirazi A, Aminyavari M, Najafi B, Rinaldi F, Razaghi M. Thermal-economic-environmental analysis and multi-objective optimization of an internal-reforming solid oxide fuel cell-gas turbine hybrid system. *International Journal of Hydrogen Energy* 2012;37:19111–24. <https://doi.org/10.1016/j.ijhydene.2012.09.143>.
- [9] Ahmadi P, Dincer I, Rosen MA. Thermodynamic modeling and multi-objective evolutionary-based optimization of a new multigeneration energy system. *Energy Conversion and Management* 2013;76:282–300. <https://doi.org/10.1016/j.enconman.2013.07.049>.
- [10] Memon AG, Memon RA, Harijan K, Uqaili MA. Thermo-environmental analysis of an open cycle gas turbine power plant with regression modeling and optimization. *Journal of the Energy Institute* 2014;87:81–8. <https://doi.org/10.1016/j.joei.2014.03.023>.
- [11] Yazdi MRM, Aliehyaei M, Rosen MA. Exergy, economic and environmental analyses of gas turbine inlet air cooling with a heat pump using a novel system configuration. *Sustainability* 2015;7:14259–86. <https://doi.org/10.3390/su71014259>.

- [12] Ehyaei MA, Tahani M, Ahmadi P, Esfandiari M. Optimization of fog inlet air cooling system for combined cycle power plants using genetic data. *Applied Thermal Engineering* 2015;76:449–61. <https://doi.org/10.1016/j.applthermaleng.2014.11.032>.
- [13] Khaljani M, Saray RK, Bahlouli K. Comprehensive analysis of energy, exergy and exergo-economic of cogeneration of heat and power in a combined gas turbine and organic Rankine cycle. *Energy Conversion and Management* 2015;97:154–65. <https://doi.org/10.1016/j.enconman.2015.02.067>.
- [14] Ahmadi A, Ehyaei M. Exergy Analysis a 5kW Polymer Electrolyte Fuel Cell (PEFC) With Cogeneration. *ASME 6th International Conference on Fuel Cell Science, Engineering and Technology: American Society of Mechanical Engineers*. 2008, p. 491–7. <https://doi.org/10.1115/FuelCell2008-65128>.
- [15] Ahmadi A, Ehyaei M. Exergy analysis of a wind turbine. *International Journal of Exergy* 2009;6:457–76. <https://doi.org/10.1504/IJEX.2009.026672>.
- [16] AliEhyaei M, Tanehkar M, Rosen MA. Analysis of an Internal Combustion Engine Using Porous Foams for thermal energy recovery. *Sustainability* 2016;8(3):267. <https://doi.org/10.3390/su8030267>.
- [17] Aliehyaei M, Atabi F, Khorshidvand M, Rosen MA. Exergy, economic and environmental analysis for simple and combined heat and power IC engines. *Sustainability* 2015;7:4411–24. <https://doi.org/10.3390/su7044411>.
- [18] Asgari E, Ehyaei M. Exergy analysis and optimisation of a wind turbine using genetic and searching datas. *International Journal of Exergy* 2015;16:293–314. <https://doi.org/10.1504/IJEX.2015.068228>
- [19] Ashari G, Ehyaei M, Mozafari A, Atabi F, Hajidavalloo E, Shalhaf S. Exergy, economic, and environmental analysis of a PEM fuel cell power system to meet electrical and thermal energy needs of residential buildings. *Journal of Fuel Cell Science and Technology* 2012;9:051001. <https://doi.org/10.1115/1.4006049>.
- [20] Z.X.Li, M.A.Ehyaei, H.KamranKasmaei, A.Ahmadi,V.Costa. Thermodynamic modeling of a novel solar powered quad generation system to meet electrical and thermal loads of residential building and syngas production. *Energy Conversion and Management* 2019;199:111982. <https://doi.org/10.1016/j.enconman.2019.111982>.
- [21] Chegini S, Ehyaei M. Economic, exergy, and the environmental analysis of the use of internal combustion engines in parallel-to-network mode for office buildings. *Journal of the Brazilian Society of Mechanical Sciences and Engineering* 2018;40:433. <https://doi.org/10.1007/s40430-018-1349-4>.
- [22] Darvish K, Ehyaei MA, Atabi F, Rosen MA. Selection of optimum working fluid for Organic Rankine Cycles by exergy and exergy-economic analyses. *Sustainability* 2015;7:15362–83. <https://doi.org/10.3390/su71115362>.
- [23] Ehyaei M, Ahmadi P, Atabi F, Heibati M, Khorshidvand M. Feasibility study of applying internal combustion engines in residential buildings by exergy, economic and environmental analysis. *Energy and Buildings* 2012;55:405–13. <https://doi.org/10.1016/j.enbuild.2012.09.002>.
- [24] Ehyaei M, Bahadori M. Internalizing the social cost of noise pollution in the cost analysis of electricity generated by wind turbines. *Wind Engineering* 2006;30:521–9. <https://doi.org/10.1260/030952406779994114>.
- [25] Ehyaei M, Bahadori M. Selection of micro turbines to meet electrical and thermal energy needs of residential buildings in Iran. *Energy and Buildings* 2007;39:1227–34. <https://doi.org/10.1016/j.enbuild.2007.01.006>.
- [26] Ehyaei M, Farshin B. Optimization of photovoltaic thermal (PV/T) hybrid collectors by genetic data in Iran's residential areas. *Advances in energy research* 2017;5:31–55. <https://doi.org/10.12989/eri.2017.5.1.031>.
- [27] Ehyaei M, Hakimzadeh S, Enadi N, Ahmadi P. Exergy, economic and environment (3E) analysis of absorption chiller inlet air cooler used in gas turbine power plants. *International Journal of Energy Research* 2012;36:486–98. <https://doi.org/10.1002/er.1814>.
- [28] Ehyaei M, Mozafari A. Energy, economic and environmental (3E) analysis of a micro gas turbine employed for on-site combined heat and power production. *Energy and Buildings* 2010;42:259–64. <https://doi.org/10.1016/j.enbuild.2009.09.001>.
- [29] Ehyaei M, Mozafari A, Ahmadi A, Esmaili P, Shayesteh M, Sarkhosh M, Dincer I. Potential use of cold thermal energy storage systems for better efficiency and cost effectiveness. *Energy and Buildings* 2010;42:2296–303. <https://doi.org/10.1016/j.enbuild.2010.07.013>.

- [30] Ehyaei M, Rosen MA. Optimization of a triple cycle based on a solid oxide fuel cell and gas and steam cycles with a multiobjective genetic data and energy, exergy and economic analyses. *Energy Conversion and Management* 2019;180:689–708. <https://doi.org/10.1016/j.enconman.2018.11.023>.
- [31] Ehyaei MA. Estimation of condensate mass flow rate during purging time in heat recovery steam generator of combined cycle power plant. *Thermal Science* 2014;18:1389–97. <https://doi.org/10.2298/tsci111031102e>.
- [32] Ehyaei MA, Anjiridezfuli A, Rosen MA. Exergetic analysis of an aircraft turbojet engine with an afterburner. *Thermal science* 2013;17:1181–94. <https://doi.org/10.2298/TSCII10911043E>
- [33] Ghasemian E, Ehyaei M. Evaluation and optimization of organic Rankine cycle (ORC) with datas NSGAI, MOPSO, and MOEA for eight coolant fluids. *International Journal of Energy and Environmental Engineering* 2018;9:39–57. <https://doi.org/10.1007/s40095-017-0251-7>.
- [34] Kazemi H, Ehyaei MA. Energy, exergy, and economic analysis of a geothermal power plant. *advances in geoenergy research* 2018;2:190–209. <https://doi.org/10.26804/ager.2018.02.07>.
- [35] Mozafari A, Ahmadi A, Ehyaei M. Optimisation of micro gas turbine by exergy, economic and environmental (3E) analysis. *International Journal of Exergy* 2010;7:1–19. <https://doi.org/10.1504/IJEX.2010.029611>
- [36] Mozafari A, Ehyaei M. Effects of regeneration heat exchanger on entropy, electricity cost, and environmental pollution produced by micro gas turbine system. *International journal of green energy* 2012;9:51–70. <https://doi.org/10.1080/15435075.2011.617021>.
- [37] Rajaei G, Atabi F, Ehyaei M. Feasibility of using biogas in a micro turbine for supplying heating, cooling and electricity for a small rural building. *Advances in energy research* 2017;5:129–145. <https://doi.org/10.12989/eri.2017.5.2.129>
- [38] Sadeghzadeh H, Aliehyaei M, Rosen MA. Optimization of a Finned Shell and Tube Heat Exchanger Using a Multi-Objective Optimization Genetic Data. *Sustainability* 2015;7:11679–95. <https://doi.org/10.3390/su70911679>.
- [39] Saidi M, Abbassi A, Ehyaei M. Exergetic optimization of a PEM fuel cell for domestic hot water heater. *Journal of Fuel Cell Science and Technology* 2005;2:284–9. <https://doi.org/10.1115/1.2041672>.
- [40] Saidi M, Ehyaei M, Abbasi A. Optimization of a combined heat and power PEFC by exergy analysis. *Journal of Power Sources* 2005;143:179–84. <https://doi.org/10.1016/j.jpowsour.2004.11.061>.
- [41] Shamoushaki M, Ehyaei M, Ghanatir F. Exergy, economic and environmental analysis and multi-objective optimization of a SOFC-GT power plant. *Energy* 2017;134:515–31. <https://doi.org/10.1016/j.energy.2017.06.058>.
- [42] Shamoushaki M, Ehyaei MA. Exergy, economic and environmental (3E) analysis of a gas turbine power plant and optimization by MOPSO data. *Thermal Science* 2018;22:2641–51. <https://doi.org/10.2298/TSCII161011091S>.
- [43] Shamoushaki M, Ghanatir F, Ehyaei M, Ahmadi A. Exergy and exergoeconomic analysis and multi-objective optimisation of gas turbine power plant by evolutionary datas. Case study: Aliabad Katoul power plant. *International Journal of Exergy* 2017;22:279–307. <https://doi.org/10.1504/IJEX.2017.083160>
- [44] Yazdi BA, Yazdi BA, Ehyaei MA, Ahmadi A. Optimization of micro combined heat and power gas turbine by genetic data. *Thermal Science* 2015;19:207–18. <https://doi.org/10.2298/TSCII121218141Y>
- [45] Yousefi M, Ehyaei M. Feasibility study of using organic Rankine and reciprocating engine systems for supplying demand loads of a residential building. *Advances in Building Energy Research* 2017;13:32–48. <https://doi.org/10.1080/17512549.2017.1354779>.
- [46] Dincer I, Rosen MA. *Exergy: energy, environment and sustainable development*: Newnes; 2012.
- [47] Valero A, Lozano MA, Serra L, Tsatsaronis G, Pisa J, Frangopoulos C, von Spakovsky MR. CGAM problem: definition and conventional solution. *Energy* 1994;19:279–86. [https://doi.org/10.1016/0360-5442\(94\)90112-0](https://doi.org/10.1016/0360-5442(94)90112-0).
- [48] Bejan A, Tsatsaronis G, Moran M, Moran MJ. *Thermal design and optimization*: John Wiley & Sons; 1996.
- [49] Seyyedi S, Ajam H, Farahat S. Thermoenviromonic optimization of gas turbine cycles with air preheat. *Proceedings of the Institution of Mechanical Engineers, Part A: Journal of Power and Energy* 2011;225:12–23. <https://doi.org/10.1177/09576509JPE959>.

- [50] Senthilkumar C, Ganesan G, Karthikeyan R. Optimization of ECM process parameters using NSGA-II. *Journal of Minerals and Materials Characterization and Engineering* 2012;11:931. <https://doi.org/10.4236/jmmce.2012.1110091>.

